Enhanced electron-phonon coupling and critical current density in rapid thermally quenched MgB_2 bulk samples

Cite as: AIP Advances **7**, 085014 (2017); https://doi.org/10.1063/1.5000259
Submitted: 03 May 2017 . Accepted: 14 August 2017 . Published Online: 25 August 2017

T. S. Suraj, M. Muralidhar, K. Sethupathi, M. S. Ramachandra Rao, and M. Murakami

Enhanced electron-phonon coupling and critical current density in rapid thermally quenched MgB_2 bulk samples

T. S. Suraj,[1] M. Muralidhar,[2,a] K. Sethupathi,[3] M. S. Ramachandra Rao,[1] and M. Murakami[2]

[1]*Department of Physics, Nano Functional Materials Technology Centre and Materials Science Research Centre, Indian Institute of Technology Madras, Chennai 600036, India*
[2]*Superconducting Materials Laboratory, Graduate School of Science and Engineering, Shibaura Institute of Technology, Tokyo 135-8548, Japan*
[3]*Department of Physics, Low Temperature Physics Laboratory, Indian Institute of Technology Madras, Chennai 600036, India*

(Received 3 May 2017; accepted 14 August 2017; published online 25 August 2017; corrected 30 August 2017)

We report Rapid Thermal Quenching (RTQ) studies on MgB_2 samples from optimized sintering temperature of 800 °C down to liquid nitrogen temperature with different sintering duration. Superior electron-phonon coupling strength ($\lambda_{e-E_{2g}}$), critical current density (J_c) and irreversibility fields (H_{irr}) compared to doped MgB_2 were observed without compromising transition temperature T_c. Structural studies showed a contraction of the unit cell due to thermal stress induced by RTQ. Enhanced $\lambda_{e-E_{2g}}$ evaluated from line width, and phonon frequency of Raman spectra using Allen equation was consistent with structural and magnetic studies. Microstructural analysis showed a decrease in grain size resulting in increased J_c and H_{irr}. [http://dx.doi.org/10.1063/1.5000259]

I. INTRODUCTION

The discovery of superconductivity at 39 K on MgB_2 by Nagamatsu *et.al* in 2001 led to a plethora of research for improving the superconducting properties of this material.[1] Because of its binary elemental composition and typically high T_c of 39 K, MgB_2 remained a potential candidate for applications in cryocooling systems, superconducting magnets and particle accelerators.[2,3] With increasing demand for high T_c superconductors in industrial applications the low-cost material processing techniques are employed and improvement in the values of J_c, T_c, H_{irr} needs to be addressed.

MgB_2 has a hexagonal crystal structure with space group P6/mmm and lattice parameters are, a = 3.084 Å and c = 3.522 Å. In this hexagonal lattice, the B atoms are arranged at each of the corners of a hexagon with three nearest neighbour B atoms in each plane and Mg atoms are positioned at the centre of the B hexagon, equidistant between successive B layers.[4] Hall measurements indicate that holes are responsible for superconductivity in MgB_2.[5] Mg atoms donate electrons to B atoms, and this results in a shift of the Fermi level, which lies nearer to the flat band resulting in Cooper pair formation. Any stress or strain in the crystal structure will be reflected in the T_c and E_{2g} band of Raman spectra of MgB_2.[6]

Among many dopants, optimizing the superconducting performance of MgB_2 materials through doping with Aluminium (Al) and Carbon (C) in various forms showed promising results in high values of J_c and H_{irr}. Slusky *et al.* reported Al doping could improve the values of J_c compared to any other dopants as it replaces Magnesium atoms, but one has to compromise the T_c drop.[7] Similarly, Carbon

[a]E-mail: miryala1@shibaura-it.ac.jp

is an effective dopant that replaces boron atoms, which are of equal atomic dimensions, and doping studies have been done using carbon in different forms, but only the values of J_c at low temperatures could be improved because of the scattering effects, and T_c drops sharply with increasing dopant concentrations.[8–11] The J_c has a strong correlation with grain size and connected grain boundaries, with various processing methods, J_c can be tuned to desired applications. Various techniques like in situ and ex-situ hot pressing, isostatic hot pressing, and high-pressure synthesis are used to produce dense MgB_2 pellets with high J_c values. All these techniques give different values in J_c and T_c which points out the control of grain size during synthesis.[12–16] In addition to this spark plasma synthesis also showed better values of J_c 8 x 10^4 A/cm^2 under 4 T field at 5 K with highly dense samples with limited porosity.[17] Nevertheless, all these high-pressure techniques are futile to be used for making large sized samples because of the restriction of the multi-anvil press. As J_c mainly depends on grain size and its connectivity and this can be controlled during the sintering process through different sintering conditions. We reported high values of J_c by optimizing sintering temperature from 775 $^\circ$C to 805 $^\circ$C and sintering duration from 1 hour –10 hours. We observed sintering temperature range from 800 $^\circ$C – 805 $^\circ$C samples for 3 hours showed the best value of J_c (270,000 A/cm^2 and 125,000 A/cm^2 (20K self-field and 1T) with nano-metric sized grains.[18]

Doping or high-pressure synthesis induced effects on J_c and T_c can be replicated through rapid thermal quenching process without compromising T_c. Defects and disorder or freezing of grain growth may happen because of the thermal stress induced during the sudden drop in temperature. Recently *Qi Cai et.al* reported quenching studies along with glycol doping to improve values of J_c. They reported high values of J_c of the order of 10^5 A/cm^2 with glycol doping and quenching.[19] The method adopted for quenching and its correlation with J_c and T_c is still unclear. Rapid thermal quenching down to LN_2 temperature induced stress and its effects on T_c and grain size in MgB_2 is not well understood. We report on a systematic investigation on rapid thermally quenched MgB_2 bulk down to LN_2 temperature with different duration of sintering and their effects on values of J_c and T_c with Raman spectra, X-ray diffraction and microstructural analysis.

II. EXPERIMENTAL

MgB_2 samples were prepared by in-situ solid state reaction in Argon (Ar) gas ambient using high purity commercial powders of Mg metal (99.9 % purity, 325 Mesh) and amorphous B (98.5% purity, submicron particles, purchased from PAVEZYUM, Advanced chemicals, Turkey). Powders were mixed in a fixed ratio of (Mg=1:2). The precursor materials of 2 grams were weighed and grounded thoroughly for 30 minutes in the glove box in Ar atmosphere to avoid oxidation. The powder was then pressed into pellets of 10 mm diameter and wrapped in Tantalum (Ta) sheets, which will prevent any oxidation during sintering. The Ta wrapped pellets were kept in a tube furnace with a continuous flow of Ar gas with a heating rate of 2 $^\circ$C/min. Samples after sintering at 800 $^\circ$C in Ar atmosphere for varying durations of 2, 3, 4 and 5 hours were rapidly quenched to LN_2 temperatures by dropping the pellets suddenly into liquid nitrogen bath. Then the samples were allowed to warm up to room temperature slowly in 1-hour duration. After the quenching process, the Ta sheets were removed, and no cracks were visible in quenched pellets. A reference MgB_2 sample was prepared under normal sintering conditions based on our optimum results with high values of J_c as we found in our earlier reports.

Phase purity and crystallinity were examined using X ray diffraction technique using high-resolution automated X-Ray diffractometer (RINT2200), with Cu-Kα radiation generated at 40 kV and 40 mA. Microstructural studies were carried out using scanning electron microscope (SEM) and atomic force microscopy (AFM). Samples were thoroughly polished in various grade SiO_2 papers for 6 hours to smoothen the surface for AFM studies.

Samples having dimensions 1.9 mm x 1.5 mm x 0.45 mm were cut from a bulk disc shaped samples with a diamond cutter and edges were polished to keep the uniformity across the dimensions. These samples were used for magnetic measurements using SQUID magnetometer (Quantum Design, model MPMS). M-H loops were traced at 20 K in applied fields ranging from 0 to 5 T. Zero Field Cooled (ZFC) M-T measurements were carried out in 10 Oe fields from 10 K to 50 K. The critical current density (J_c) values at 20 K were estimated using Beans critical state model equation

$$J_c = \frac{20\Delta m}{a^2 d\,(b - \frac{a}{3})} \tag{1}$$

Where a, b and d represents the cross sectional dimensions (b ≥ a) and thickness of the sample respectively (in mm) and ∆m is the difference in magnetic moment values during increasing and decreasing fields of the hysteresis loop in first and second quadrant.[20] Room temperature Raman spectroscopy studies were carried out in all four RTQ samples using Horiba Raman spectrometer at 532 nm excitation wavelength with 1800 grating monochromator.

III. RESULTS AND DISCUSSIONS

A. Rapid thermal quenching

This technique retains the mechanical performance of the rapid thermally quenched samples as the same process through without quenching. We speculated the sudden freezing of grains might happen if the temperature varies rapidly from 800 °C to liquid nitrogen temperature (-196°C). This was evident in our micro structural observations through SEM and AFM. Smaller grains of less than 80 nm was observed with better connectivity than slowly cooled samples. This is clearly in agreement with the magnetic values of J_c and H_{irr}. The values of T_c also varied with sintering duration, and we could optimize the best sintering temperature to be 800 °C.

B. X-ray diffraction

The XRD analysis of the normally cooled MgB_2 sample and rapid thermally quenched samples are presented in Fig.1 (left). The figure clearly depicts the phase purity of MgB_2 samples, and no traces of Mg and B precursor impurity peaks were noticed. It is well understood from the data that even though the quenching happens at 800 °C, all reactions take place during 600 °C–800 °C duration. As it is inevitable a little trace of MgO were observed which is consistent with literature.[21] As speculated, the stress created in the RTQ samples was evident in X ray diffraction data with a slight shift in (100) peak towards higher angle compared to a reference sample, which is shown in Fig.1 (right). The a-axis lattice parameter has been changed considerably due to thermal stress induced due to this quenching process. The lattice parameter of *a*- axis for 3 hours rapid thermally quenched sample contracted compared to normally sintered sample. A shift of 0.00231 Å is recorded for a - axis. (fig 1 right, inset). The samples sintered for 2 hours and 3 hours had slight shifts in lattice parameter, and sample sintered for 5 hours remained the same as the normally sintered sample. This kind of lattice contraction was reported for C doped sample where carbon substitution resulted in changes in T_c and J_c.[6] Compared to other samples the 3 hours sintered sample showed sharp T_c, and this behaviour could be attributed to the contraction of the unit cell due to rapid thermal quenching

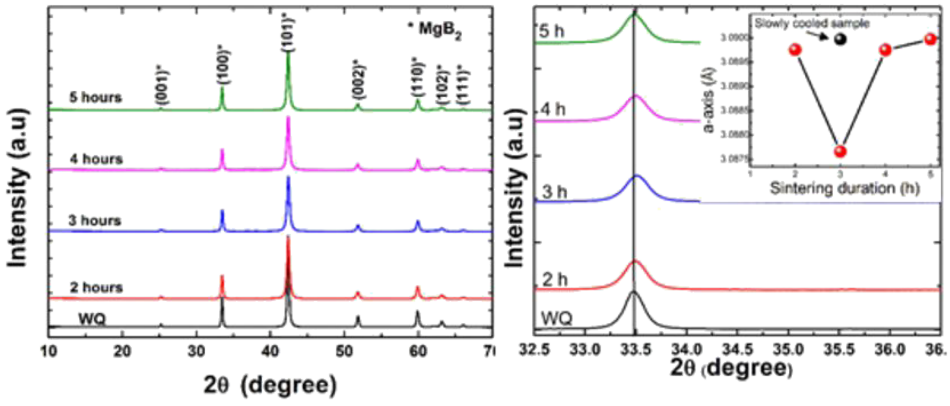

FIG. 1. X-ray diffraction spectra of rapid thermally quenched (RTQ) samples with different duration in sintering starting from 2 to 5 hours sintered sample with 1hr interval and without quenched (WQ) sample. All samples were synthesized in Ar atmosphere to avoid oxidation (left); The shift in (100) peak of rapid thermally quenched (RTQ) sample and without quenched (WQ) samples with different duration in sintering (right). WQ sample peak is kept as a reference. Inset image shows the a-axis lattice parameter variation with different duration in sintering and compared with WQ samples.

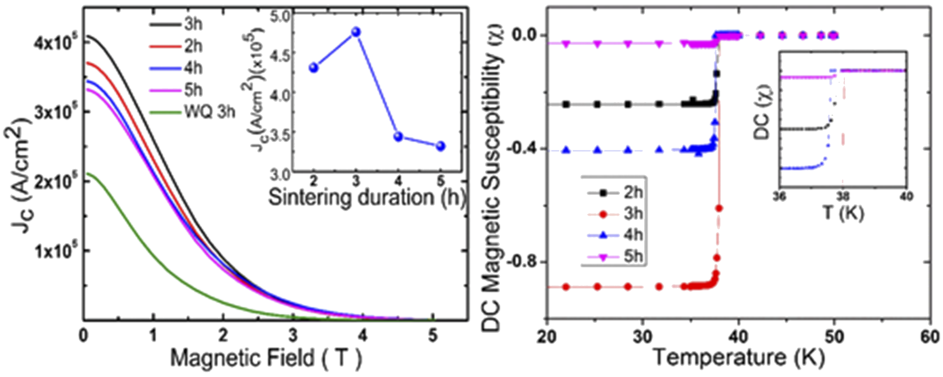

FIG. 2. Sintering duration versus critical current density J_c for RTQ MgB_2 and WQ samples obtained from M-H loop using extended Beans critical state model (left). The measurement was done at 20 K. The inset shows J_c variation with duration of sintering; DC magnetic susceptibility plotted with temperature shows the critical temperature T_c for RTQ samples (right). The inset shows enlarged image at T_c.

process. In Raman spectra, the changes in E_{2g} mode is consistent with this observation while the c-axis remained constant for all set of samples.

C. Magnetic characterization

The values of critical current density J_c were estimated based on the extended Beans critical state model from the magnetization hysteresis loops by applying magnetic fields from -1 T to 5 T at 20 K using a SQUID magnetometer. Fig.2 (left) shows the values of J_c v/s magnetic field. The significant increase in the value of J_c on quenched samples compared to the reference sample is attributed to the sudden arrest of grains of an average size of 80 nm and increased grain connectivity. On increasing the duration of sintering duration for more than 3 hours, the value of J_c was found to be decreasing with degrading T_c as shown in Fig 2 (left). While reducing sintering duration from 3 hours the same trend was observed but with a slight reduction in J_c values. The T_c values (fig 2 right, inset) show a drop when it is deviating from 3 hours sintered sample. Higher values of J_c can only be achieved through doping which will alter the T_c. Without changing the T_c, we were successful in optimizing the sintering conditions to 3 hours. The T_c value also shows the 3 hours sintered sample retained highest T_c among the other samples. The sharp transition temperature observed for 3 hours sintered sample is consistent with Raman and XRD data. To study the flux pinning behaviour in RTQ samples the normalized volume pinning force density f_p ($f_p = F_p / F_{p,max}$) is plotted against reduced field h ($h=H/H_{irr}$) at 20 K (fig 3). The irreversibility field H_{irr} was determined from the magnetization hysteresis loops using the criterion of 100 A/cm^2. The flux pinning data shows (fig 3) a shift to the high field region, which is an indicator of stress, induced disorder in the system and this confirms the

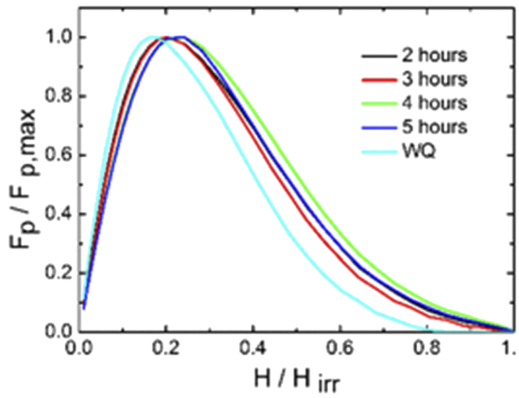

FIG. 3. Normalized flux pinning density (f) plotted against reduced field (h) shows the increased flux pinning behaviour in RTQ samples.

shift of B_{1g} peak in Raman spectra. Even with increasing the sintering temperature, the peak shifts towards the high field region. The reduced field value $h = 0.23$ shows dominant pinning centres are due to defects or disorder induced during the thermal stress which was evident from XRD data and Raman spectra.

D. Raman spectroscopy study

Group theory predicts four optical vibrational modes for the space group P6/mmm at the Γ point in the Brillouin zone for which MgB_2 belongs. They are the E_{2g} Raman mode (~600 cm^{-1}), silent B_{1g} mode (~700 cm^{-1}), A_{2u} (~400 cm^{-1}) mode and the infrared-active E_{1u} (~330 $cm^{-1)}$ mode.[22] According to Motaman *et.al* the in-plane atomic vibrations of boron atoms is responsible for the origin of the E_{2g} band and these vibrations couples with σ electronic bands to show superconductivity in MgB_2.[23] Thus, the E_{2g} phonon mode is highly sensitive to intrinsic defects or lattice distortions due to chemical pressure induced by dopants. Any E_{2g} phonon mode changes will be reflected in $T_{c,}$ and it is well studied in the literature.[24,25] There are reports on precursor material being a dependent factor in deciding the position of E_{2g} mode.[25] As stated earlier we used nano boron from PAVEZYUM, Advanced chemicals, Turkey which has a distinct signature in Raman spectrum due to its size effect. Compared to bulk MgB_2 prepared with crystalline boron (wave number <590–660cm^{-1}) and MgB_2 synthesized with nano boron (wave number ~ 573 cm^{-1}) the precursor shows a different E_{2g} shift. This is because of the change in shape of the Fermi surface of MgB_2 due to increased Mg vacancy concentrations that introduces defect scattering and band filling effects which result in reduced density of states.[26]

In this study, we have obtained Raman spectra (fig 4, top left) for RTQ samples and compared it with normally sintered MgB_2 samples. As discussed above we have used nano boron, and the E_{2g}

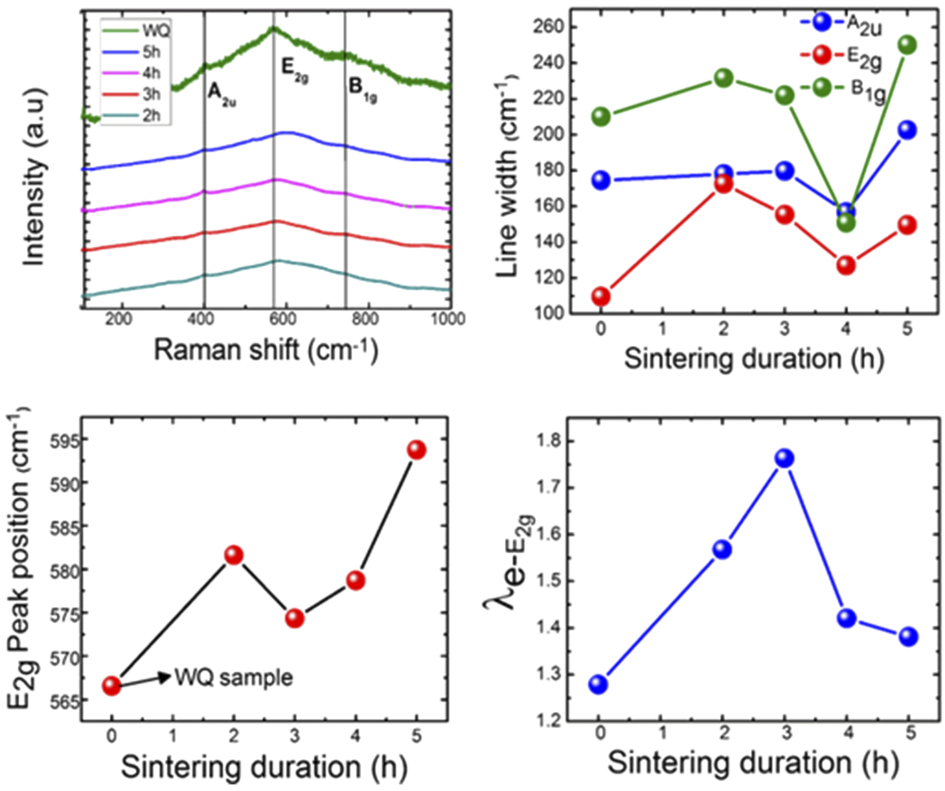

FIG. 4. Room temperature Raman spectra of RTQ and WQ samples. The E_{2g}, A_{2u} and B_{1g} represents the vibrational modes in the MgB_2 sample, WQ sample spectra is kept as a reference (line) (top left); The E_{2g} peak shift for RTQ and WQ samples is represented with varying duration of sintering (bottom, left); The FWHM of all the three modes were obtained from Gaussian fitting of Raman peaks, and are plotted with duration of sintering (top right); E_{2g} phonon – electron coupling strength $\lambda_{e\text{-}E2g}$ versus sintering duration is plotted for RTQ samples (bottom right).

and other peak shifts are evident (Fig 4, bottom left). The T_c values obtained from the magnetic data is in good agreement with our E_{2g} mode shift. The 3 hours annealed and quenched sample showed a sharp T_c which reflects the lower disorder and stress induced in the system while the 4 and 5 hours sintered samples shows red shift because of inherent disorder induced in the system due to prolonged heating and thermal stress because of rapid quenching.

The Raman spectra of all the samples were fitted with three broad Gaussian peaks corresponding to the three modes. The FWHM (fig.4, top right) of E_{2g} peak gives the electron phonon coupling strength. The red shift of E_{2g} peak results in weak E_{2g} phonon modes-electron coupling, and it can adversely affect the T_c value. Gaussian fitting obtains Line width. In our case, the increase in the shift of E_{2g} peak for rapidly quenched samples compared to without quenched samples shows the reduction in T_c. The 3 hours sintered sample showed a sudden decrease in E_{2g} peak relative to the trend followed for other long duration sintered samples, and it was reflected in the sharp T_c alone for this sample. So our Raman E_{2g} shift is consistent with T_c data.

To further understand the role of electron-E_{2g} coupling with sintering duration, which affected T_c, we estimated the electron-E_{2g} phonon coupling strength using Allen equation. This equation is a better tool to relate the phonon frequency (ω) and Linewidth (Γ) with electron-E_{2g} phonon coupling strength ($\lambda_{e-E_{2g}}$).[27,28]

$$\lambda_{e-E_{2g}} = \frac{\Gamma}{2\pi N(0)\omega^2} \tag{2}$$

Where $\lambda_{e-E_{2g}}$ is the electron-E_{2g} phonon coupling strength. *N(0)* is density of states DOS (states/eV cell spin) on the Fermi surface. Γ represents the Linewidth and ω is phonon frequency corresponding to Raman active E_{2g} mode. *N (0)* for pure MgB_2 is 0.0354 states/eV cell spin.[28] The $\lambda_{e-E_{2g}}$ values were plotted against the duration of sintering (fig.4, bottom right). In our rapid, thermally quenched samples the 3 hours sintered samples show enhanced $\lambda_{e-E_{2g}}$ compared to all other samples and this shows the reason for sharp values of T_c because of improved E_{2g} phonon-electron coupling strength. All other samples showed a decline in coupling strength, and it was reflected in the T_c data (fig 2 right, inset).

The B_{1g} peak line width (see fig 4, top right) provides information about phonon density of states (PDOS) and is related to the disorder or distortion present in the lattice.[29] The red shift of this mode will correspond to compressive stress and the blue shift, which will be due to the tensile stress.[30,31] With the increase in duration of sintering time with the peak position decreases down to 3 hours sintered sample and found an abrupt decrease in 4 h sintered case with a sudden jump for 5 hours sintered sample. This might be due to the compressive stress induced in the system, which is consistent with XRD data of 3 h sintered sample. Thus the extra strain induced during thermal transition might lead to improved values of J_c and H_{irr}.[32] A_{2u} mode does not show significant changes with duration in sintering except for 4 hours sintered sample.

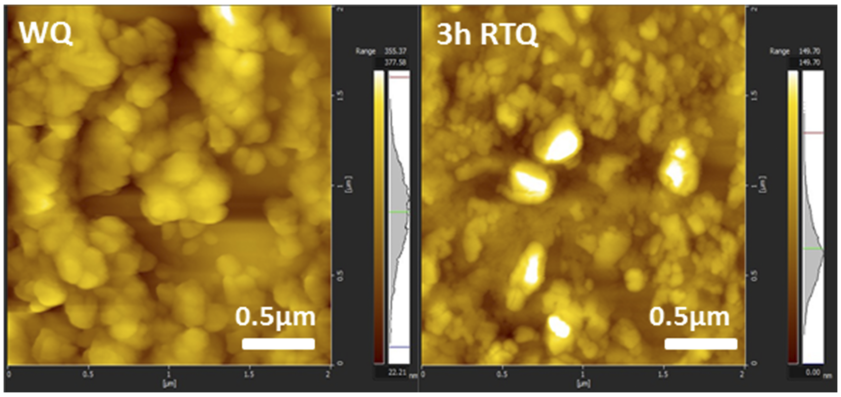

FIG. 5. shows AFM images of 2mic X 2mic size of RTQ and WQ samples with different duration in sintering.

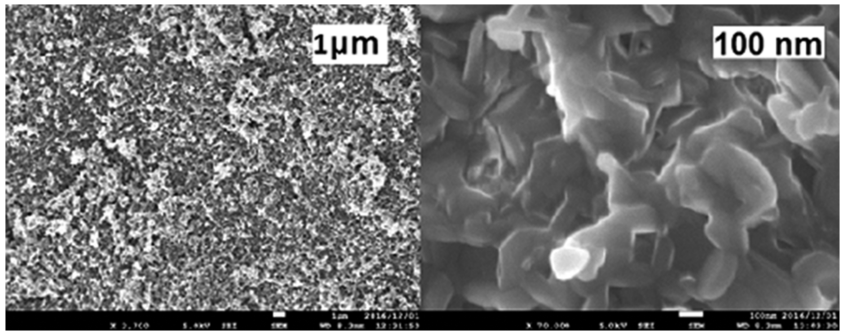

FIG. 6. SEM images of 3hours RTQ samples in 1 µm and 100 nm magnification.

E. Microstructural analysis

The increase in critical current density J_c is correlated with the change in grain boundaries and grain sizes. Rapid thermal quenching process affected the microstructure by arresting the growth of grains. We have estimated the microstructure through scanning electron microscopy (SEM) and atomic force microscopy (AFM). Through SEM images it was difficult to distinguish between grains so we have used AFM to estimate the grain size. Line profile data acquired using AFM showed the grain size diminishes for RTQ processed samples (not shown).

AFM images were recorded at 2 µm x 2 µm scales to observe the grain size. (Fig 5). The grain size found to be decreasing for 3 hours quenched sample compared to the reference one. Grains with size less than 100 nm is predominant in this optimum sample. Line profile data also confirmed the counts of grains in this range. Grain size and the values of J_c have an inverse relation, in our case also the lower grain size corresponding to 3 hours sintered samples shows best values of J_c among all samples.

SEM images at low and high magnification were observed (fig 6). This provided us with a confirmatory data to AFM analysis. The dependence of J_c values on the micro structure is well studied, and it increases with optimized grain size. Our rapidly quenched samples showed an increase in values of J_c due to decreased grain size. The porosity and connectivity of the grains can be investigated to get further insight into the increase of J_c.

IV. CONCLUSION

We have investigated rapid thermal quenching (RTQ) studies on bulk MgB_2 samples down to LN_2 temperature. The 3 hours sintered and quenched sample showed superior J_c values of 4.8 x 10^5 A/cm ^{2} and sharp T_c at 38.1 K. The sharp value of T_c is attributed to contraction of the unit cell, which was confirmed by XRD and Raman spectra. To get further insight into this sharp drop in T_c, we evaluated the electron phonon coupling strength $\lambda_{e-E_{2g}}$ of E_{2g} mode using Allen equation with line width and phonon frequency from Raman spectra. The 3 hours sintered sample retained high E_{2g}-electron coupling which is consistent with our sharp T_c values of 38.1 K. Microstructural observations confirmed the reduced grain size attributed to enhanced J_c values in rapid thermally quenched samples. The compressive stress induced disorder was visible on the B_{1g} peak of Raman spectra; this could be another reason for the substantial increase in the value of J_c.

ACKNOWLEDGMENTS

The work was supported by Japan Student Services Organization (JASSO), Shibaura Institute of Technology (SIT) under the Top Global University Project, Designed by Ministry of Education, Culture, Sports, Science and Technology in Japan.

[1] J. Nagamatsu, N. Nakagawa, T. Muranaka, Y. Zenitani, and J. Akimitsu, Nature **410**, 63 (2001).
[2] A. Yamamoto, A. Ishihara, M. Tomita, and K. Kishio, Appl. Phys. Lett. **105**, 032601 (2014).
[3] A. B. Abrahamsen, N. Zangenberg, A. Baurichter, J.-C. Grivel, and N. H. Andersen. Denmark Forskningscenter Risoe. Risoe-R, No. 1578(EN), (2006).

[4] M. E. Jones and R. E. Marsh, J. Am. Chem. Soc. **76**, 1434 (1954).
[5] W. N. Kang, C. U. Jung, K. H. P. Kim, M. S. Park, S. Y. Lee, H. J. Kim, E. M. Choi, K. H. Kim, M. S. Kim, and S. L. Lee, Appl. Phys. Lett. **79**, 982 (2001).
[6] C. Li and L. Hua, Chin. Phys. Lett. **20**(7), 1128 (2003).
[7] J. S. Slusky, N. Rogado, K. A. Regan, M. A. Hayward, P. Khalifah, T. He, and R. J. Cava, Nature **410**, 343 (2001).
[8] S. X. Dou, W. K. Yeoh, J. Horvat, and M. Ionescu, Appl. Phys. Lett. **83**, 4996–4998 (2003).
[9] W. K. Yeoh, J. H. Kim, J. Horvat, X. Xu, M. J. Qin, and S. X. Dou, Supercond. Sci. Technol. **19**, 596–599 (2006).
[10] J. H. Kim, S. Zhou, M. S. A. Hossain, A. V. Pan, and S. X. Dou, Appl. Phys. Lett. **89**, 142505 (2006).
[11] M. S. A. Hossain, C. Senatore, R. Flükiger, M. A. Rindfleisch, M. J. Tomsic, and J. H. Kim, Supercond. Sci and Tech. **22**, 095004 (2009).
[12] A. Handstein, D. Hinz, G. Fuchs, K. H. Muller, K. Nenkov, O. Gutfleisch, V. N. Narozhnyi, and L. Schultz, J. Alloys Comp. **329**, 285–289 (2001).
[13] T. C. Shields, K. Kawano, D. Holdom, and J. S. Abell, Supercond. Sci and Tech. **15**, 202–205 (2002).
[14] C. U. Jung, M.-S. Park, W. N. Kang, M.-S. Kim, K. H. P. Kim, S. Y. Lee, and S.-I. Lee, Appl. Phys. Lett. **78**(26), 4157–4159 (2001).
[15] C. Q. Jin, S. C. Li, J. L. Zhu, F. Y. Li, Z. X. Liu, and R. C. Yu, J. Mater. Res. **17**(3), 525 (2002).
[16] D. C. Larbalestier, L. D. Cooley, M. O. Rikel, A. A. Polyanskii, J. Jiang, S. Patnaik, X. Y. Cai, D. M. Feldmann, A. Gurevich, A. A. Squitieri, M. T. Naus, C. B. Eom, E. E. Hellstrom, R. J. Cava, K. A. Regan, N. Rogado, M. A. Hayward, T. He, J. S. Slusky, P. Khalifah, K. Inumaru, and M. Haas, Nature **410**, 186–189 (2001).
[17] S. H. Shim, K. B. Shim, and J.-W. Yoon, J. Am. Ceram. Soc. **88**(4), 858–861 (2005).
[18] M. Muralidhar, K. Nozaki, H. Kobayashi, X. L. Zeng, A. Koblischka Veneva, M. R. Koblischka, K. Inoue, and M. Murakami, J. Alloys Compd. **649** (2015).
[19] Q. Cai, Z. Ma, Y. Liu, Q. Guo, J. Xiong, H. Li, and F. Qin, J. Mater. Sci. Mater. Electron. **27**(9), 9431–9436 (2016).
[20] D. X. Chen and R. B. Goldfarb, J. Appl. Phys. **66**, 2489–2500 (1989).
[21] A. Bateni, S. Repp, R. Thomann, S. Acar, E. Erdem, and M. Somer, Appl. Phys. Lett. **105**, 202605 (2014).
[22] T. P. Devereaux and R. Hackl, Rev. Mod. Phys. **75**, 175, 11 (2007).
[23] A. Motaman, M. S. A. Hossain, X. Xu, K. W. See, K. C. Chung, and S. X. Dou, Supercond. Sci. and Tech. **26**, 085013 (2013).
[24] A. Bateni, E. Erdem, S. Repp, S. Acar, I. Kokal, W. Häßler, S. Weber, and M. Somer, J. Appl. Phys. **117**, 153905 (2015).
[25] A. Bateni, E. Erdem, S. Repp, S. Weber, and M. Somer, Appl. Phys. Lett. **108**, 202601 (2016).
[26] Bateni, S. Repp, R. Thomann, S. Acar, E. Erdem, and M. Somer, Appl. Phys. Lett. **105**, 202605 (2014).
[27] P. B. Allen, Phys. Rev. B **6**, 2577 (1972).
[28] A. Shukla, M. Calandra, M. d'Astuto, M. Lazzeri, F. Mauri, C. Bellin, M. Krisch, J. Karpinski, S. M. Kazakov, J. Jun, D. Daghero, and K. Parlinski, Phys. Rev. Lett. **90**, 095506 (2003).
[29] K. P. Bohnen, R. Heid, and B. Renker, Phys. Rev. Lett. **86**, 5771 (2001).
[30] Paillard, P. Puech, R. Sirvin, S. Hamma, and P. R. I. Cabarrocas, J. Appl. Phys. **90**, 3276 (2001).
[31] W. X. Li, Y. Li, R. H. Chen, R. Zeng, S. X. Dou, M. Y. Zhu, and H. M. Jin, Phys. Rev. B **77**, 094517 (2008).
[32] R. Zeng, S. X. Dou, L. Lu, W. X. Li, J. H. Kim, P. Munroe, R. K. Zheng, and S. P. Ringer, Appl. Phys. Lett. **94**, 042510 (2009).